

Pion condensation at lower than physical quark masses

Bastian B. Brandt,^a Volodymyr Chelnokov,^{b,*} Francesca Cuteri^b and Gergely Endrődi^a

^a*Institute for Theoretical Physics, University of Bielefeld,
D-33615 Bielefeld, Germany*

^b*Institut für Theoretische Physik, Goethe-Universität Frankfurt
Max-von-Laue-Str. 1, 60438 Frankfurt am Main, Germany*

*E-mail: brandt@physik.uni-bielefeld.de, chelnokov@itp.uni-frankfurt.de,
cuteri@itp.uni-frankfurt.de, endrodi@physik.uni-bielefeld.de*

In QCD at large enough isospin chemical potential Bose-Einstein Condensation (BEC) takes place, separated from the normal phase by a phase transition. From previous studies the location of the BEC line at the physical point is known. In the chiral limit the condensation happens already at infinitesimally small isospin chemical potential for zero temperature according to chiral perturbation theory. The thermal chiral transition at zero density might then be affected, depending on the shape of the BEC boundary, by its proximity. As a first step towards the chiral limit, we perform simulations of 2+1 flavors QCD at half the physical quark masses. The position of the BEC transition is then extracted and compared with the results at physical masses.

*The 39th International Symposium on Lattice Field Theory (Lattice2022),
8-13 August, 2022
Bonn, Germany*

*Speaker

1. Introduction

The phase structure of QCD continues to be an object of great interest for both experimental and theoretical studies. There is currently a wealth of numerical simulation results at zero quark density, from which we know, in particular, that the chiral symmetry restoration at physical quark masses is a continuous crossover [1]. Studying the theory in the chiral limit is complicated by the appearance of zero modes of the Dirac operator, and the need to go to the continuum limit to restore chiral symmetry with Wilson or staggered fermions, or to employ computationally much costlier chiral symmetric fermion discretizations. Nevertheless, there is a recent progress in this region which, in particular, suggests that in the limit $m_{\text{ud}} = 0$ the chiral transition is of second order (for $N_f = 2, 3$) and becomes a crossover at arbitrarily small nonzero quark masses [2].

Extending the QCD phase diagram to nonzero densities is confounded by the sign problem – the Boltzmann weight of the lattice configuration becomes complex at nonzero μ_B , preventing straightforward use of importance sampling. Different ways to overcome this problem were proposed (see [3, 4] for a review), but still the problem is far from being solved.

Another possible extension of the QCD phase diagram is to the region of nonzero isospin density at $\mu_I \neq 0$, potentially relevant for early Universe cosmology [5], for instance. At pure isospin chemical potential $\mu_I \neq 0$, $\mu_B = 0$, the theory is sign problem-free and the standard Monte-Carlo simulations can be performed [6]. The recent study [7] shows that the deconfinement transition remains a crossover for $\mu_I \leq m_\pi/2$, until it intersects with the second order pion condensation line, which is found to be approximately vertical at small enough T (see Figure 1). The μ_I - T plane can also be used to check the methods targeted at studying QCD at finite μ_B – since we can compare

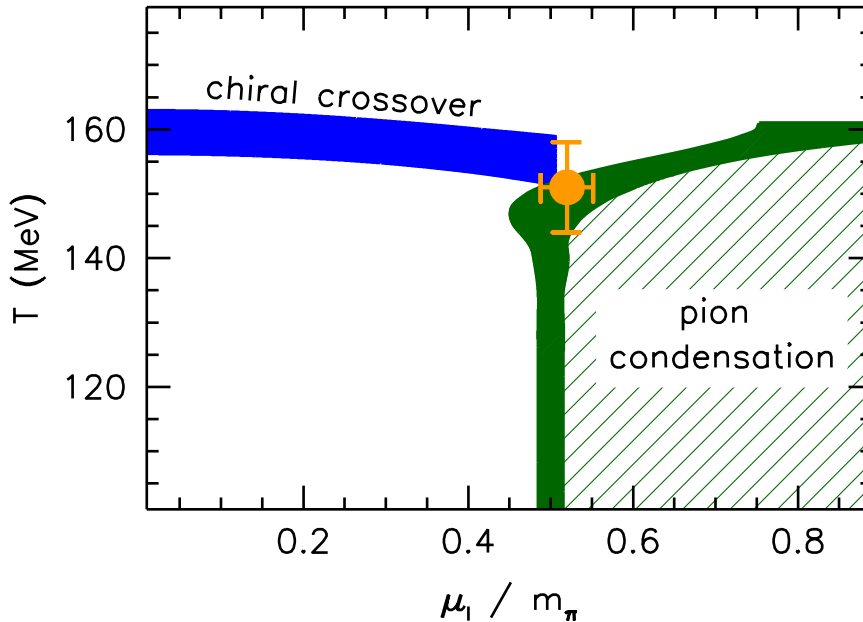


Figure 1: The QCD phase diagram in T - μ_I plane at physical quark masses, obtained in [7].

their results with the results of direct simulation, that is possible here [8]. Additionally, the ability to numerically sample the theory in the μ_I - T plane can be exploited to perform the reweighting to nonzero μ_B [9].

The phase diagram shown in Figure 1 has an interesting implication concerning the chiral phase diagram. At zero temperature, the pion condensation happens at $\mu_I = m_\pi/2$. When the light quark mass goes to zero, the pion mass also goes to zero as $m_\pi \sim \sqrt{m_{ud}}$ according to chiral perturbation theory. Thus at least at zero temperature in the chiral limit pion condensation happens already at arbitrarily small isospin chemical potential. From Figure 1 we see that at physical mass the isospin transition line remains vertical up until it meets the chiral crossover line. If that holds also at $m_{ud} = 0$, then in the chiral limit the pion condensation line would lie on the $\mu_I = 0$ axis up to $T = T_c$ – i.e. up to the chiral phase transition temperature. In this scenario the pion condensate in the chiral limit at $T = T_c$ exists at arbitrarily small isospin chemical potential, affecting the chiral phase transition at zero chemical potential (Figure 2, left). Alternatively, the phase transition line can start bending towards larger μ_I as the quark masses are reduced, resulting in a different phase structure (Figure 2, right). Previous studies using the Nambu-Jona-Lasinio model [10], as well as the functional renormalization group [11], support the first phase picture. To verify this, direct Monte Carlo QCD simulations are necessary.

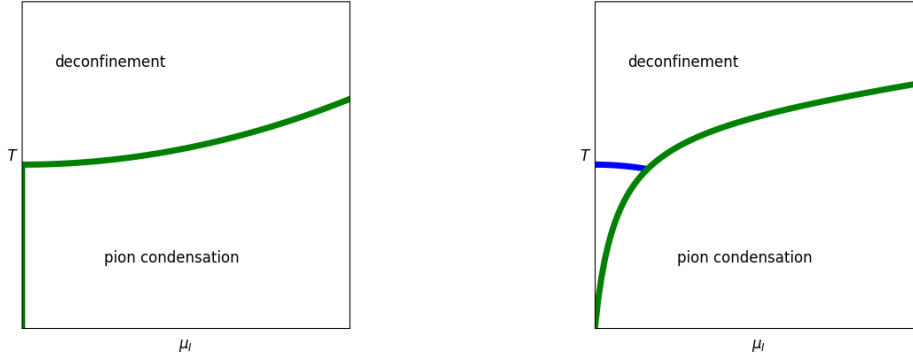


Figure 2: Two possibilities for the phase diagram in T - μ_I plane at the chiral limit.

As a first step, in this work we perform the simulation of QCD at nonzero isospin density for $m_{ud} = m_{ud,phys}/2$, comparing the position of the pion condensation transition with the results at physical masses at a series of temperatures.

2. Simulation setup

We study 2 + 1-flavour QCD using staggered fermions on a $24^3 \times 8$ lattice. The setup is the same as the one used in [7], with the light quark masses changed to half their physical value. The partition function of the theory has the form

$$\mathcal{Z} = \int \mathcal{D}U_\mu e^{-\beta S_G} (\det \mathcal{M}_{ud})^{1/4} (\det \mathcal{M}_s)^{1/4}, \quad (1)$$

where S_G is the tree-level Symanzik improved gauge action, \mathcal{M}_{ud} and \mathcal{M}_s are, correspondingly, light and strange quark matrices

$$\mathcal{M}_{ud} = \begin{pmatrix} \mathcal{D}(\mu_I) + m_{ud} & \lambda\eta_5 \\ -\lambda\eta_5 & \mathcal{D}(-\mu_I) + m_{ud} \end{pmatrix}, \quad \mathcal{M}_s = \mathcal{D}(0) + m_s. \quad (2)$$

Here λ is a pion source term which explicitly breaks the $U_{\tau_3}(1)$ symmetry of the action, which both allows us to see the pion condensate on the finite volume lattice, and, at the same time, improves the condition number of the light quark matrix. To get physically meaningful results, the limit $\lambda \rightarrow 0$ must be taken.

The Boltzmann weight defined by (1) is positive, which is obvious for the gauge action and the strange quark determinant. The positiveness of the light quark determinant follows from the generalized η_5 -hermiticity relation that the Dirac operator satisfies,

$$\eta_5 \mathcal{D}(-\mu_I) \eta_5 = \mathcal{D}(\mu_I)^\dagger. \quad (3)$$

Now, taking the matrix $B = \text{diag}(1, \eta_5)$ in flavour space, that has a unit determinant, we get

$$B\mathcal{M}_{ud}B = \begin{pmatrix} \mathcal{D}(\mu_I) + m_{ud} & \lambda \\ -\lambda & (\mathcal{D}(\mu_I) + m_{ud})^\dagger \end{pmatrix},$$

$$\det \mathcal{M}_{ud} = \det (B\mathcal{M}_{ud}B) = \det \left(|\mathcal{D}(\mu_I) + m_{ud}|^2 + \lambda^2 \right) > 0. \quad (4)$$

To locate the pion condensation onset, we measure the pion condensate

$$\Sigma_\pi = \frac{m_{ud}}{m_\pi^2 f_\pi^2} \langle \pi^\pm \rangle, \quad (5)$$

$$\langle \pi^\pm \rangle = \frac{T}{V} \frac{\partial \log \mathcal{Z}}{\partial \lambda} = \frac{T}{2V} \left\langle \text{Tr} \frac{\lambda}{|\mathcal{D}(\mu_I) + m_{ud}|^2 + \lambda^2} \right\rangle, \quad (6)$$

where the trace can be calculated using noisy estimators. The multiplicative renormalization term in (5) depends on the light quark mass m_{ud} , the pion mass m_π that corresponds to m_{ud} , and the pion decay constant f_π . The chiral perturbation theory predicts that $m_\pi \sim \sqrt{m_{ud}}$ when the light quark mass goes to zero, so assuming this relation holds for physical light quark mass we can approximate the renormalization (5) as

$$\Sigma_\pi = \frac{m_{ud,phys}}{m_{\pi,phys}^2 f_\pi^2} \langle \pi^\pm \rangle, \quad (7)$$

where $m_{ud,phys}$ and $m_{\pi,phys}$ are physical light quark and pion masses.

The pion condensate estimated using Eq. (5) at $T = 114$ MeV, for three different values of λ can be seen in Figure 3. We see that even for the smallest value of λ we are still far from the limiting regime $\lambda \rightarrow 0$. Unfortunately, the simulations at smaller λ values become prohibitively expensive due to very large condition numbers of the light quark matrix, that causes a sharp increase of iterations needed for matrix inversion. At even smaller λ values this results in a loss of convergence of the conjugate gradient method.

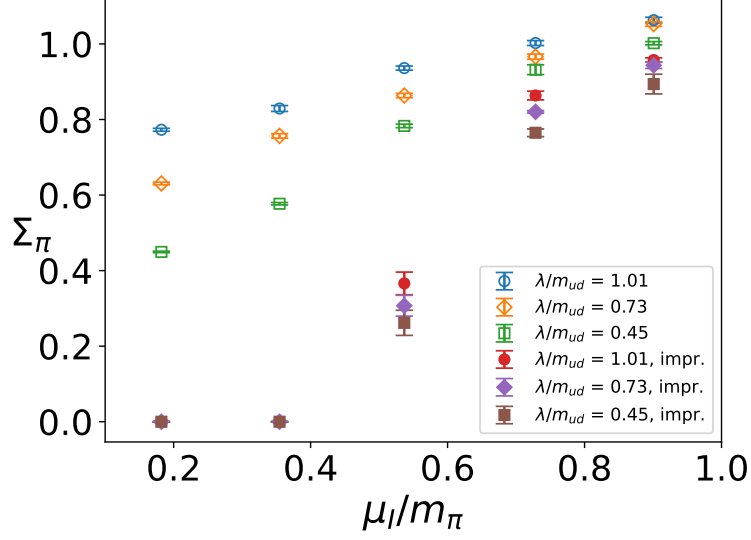


Figure 3: Comparison of the improved and the unimproved pion condensate at $T = 114$ MeV for three different values of λ .

3. Improved pion condensate

We can improve the convergence to the $\lambda \rightarrow 0$ limit by using the Banks-Casher type relation for the pion condensate (6), that was obtained in [7]

$$\langle \pi^\pm \rangle = \frac{T}{2V} \left\langle \text{Tr} \frac{\lambda}{|\not{D}(\mu_I) + m_{ud}|^2 + \lambda^2} \right\rangle = \frac{T}{2V} \left\langle \sum_n \frac{\lambda}{\xi_n^2 + \lambda^2} \right\rangle, \quad (8)$$

where ξ_n is the n -th singular value of the Dirac operator:

$$(\not{D}(\mu_I) + m_{ud})^\dagger (\not{D}(\mu_I) + m_{ud}) \phi_n = \xi_n^2 \phi_n. \quad (9)$$

In the infinite volume limit, the summation can be replaced by integration

$$\langle \pi^\pm \rangle = \frac{\lambda}{2} \left\langle \int d\xi \rho(\xi) (\xi^2 + \lambda^2)^{-1} \right\rangle, \quad (10)$$

and taking the limit $\lambda \rightarrow 0$ we get

$$\langle \pi^\pm \rangle = \frac{\pi}{4} \langle \rho(0) \rangle. \quad (11)$$

Thus, the limit $\lambda \rightarrow 0$ of the pion condensate is proportional to the singular value density at zero. Due to the finite size of the lattice the singular values form a discrete set, but we can approximate the density by calculating the fraction of the singular values lying in the interval $[0, \xi]$, and then extrapolating to $\xi = 0$

$$\rho(0) = \frac{T}{V} \lim_{\xi \rightarrow 0} \frac{n(\xi)}{\xi}, \quad (12)$$

The behavior of such ‘‘averaged densities’’ for three regimes – finite spectral gap at $\mu_I/m_\pi < 0.5$, $\rho(0) \approx 0$ at $\mu_I/m_\pi \approx 0.5$, and $\rho(0) > 0$ at $\mu_I/m_\pi > 0.5$, is shown on Figure 4.

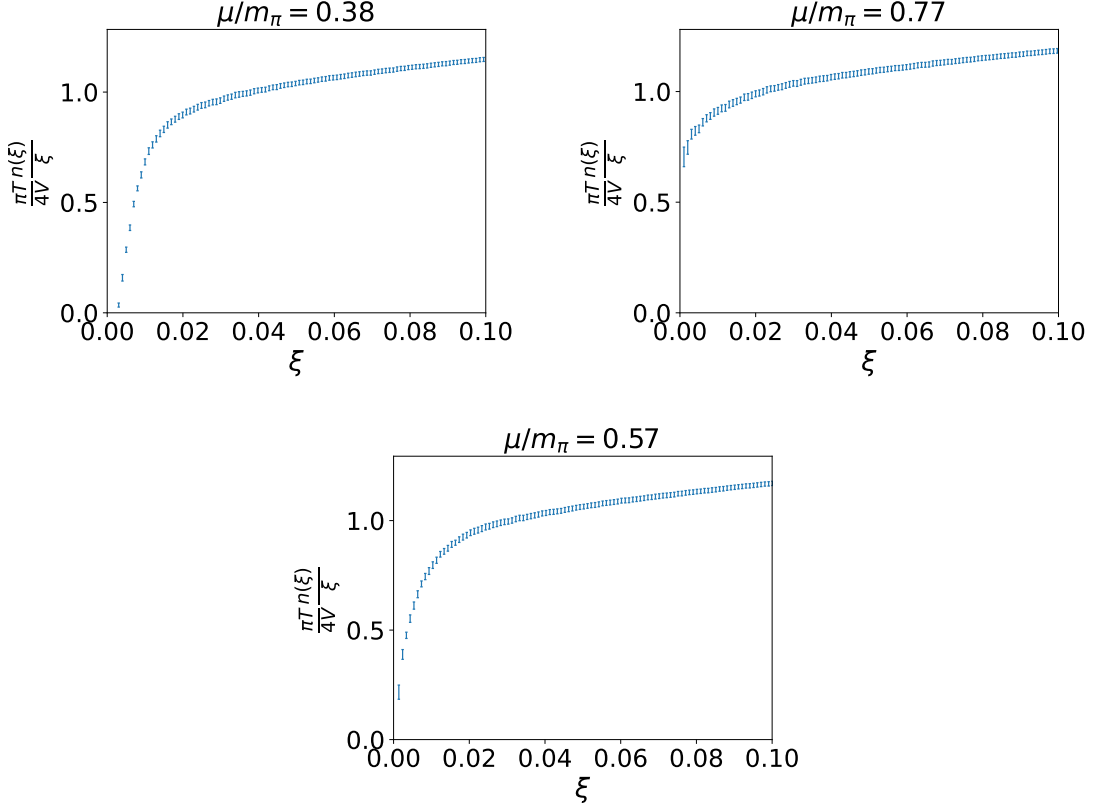


Figure 4: The integrated spectral density dependence on the integration region ξ for $\mu_I/m_\pi < 0.5$ (left), $\mu_I/m_\pi > 0.5$ (right), and $\mu_I/m_\pi \approx 0.5$ (bottom) ($T = 132$ MeV).

To perform the extrapolation to $\xi = 0$ we perform a polynomial fit of the integrated spectral density in a given region, obtaining a value of $\langle \rho(0) \rangle$ and then take a weighted median of all the fit results with the weight $\exp(-\chi_r^2)$, where χ_r^2 is the (correlated) chi-squared statistic of the fit per degree of freedom. The error estimate of $\langle \rho(0) \rangle$ is then taken as a value $\Delta\rho$, for which the interval $[\langle \rho(0) \rangle - \Delta\rho, \langle \rho(0) \rangle + \Delta\rho]$ contains 0.68 of the total weight of the estimates.

We can further improve the convergence of the improved pion condensate observable to the limit $\lambda \rightarrow 0$ by approximating $\langle \rho(0) \rangle_0$ (the expectation value of $\rho(0)$ with respect to the $\lambda = 0$ partition function) using the leading order reweighting, expanding the Boltzmann weight of a given configuration in a Taylor series in λ ,

$$\langle \rho(0) \rangle_0 = \frac{\langle \rho(0) W(\lambda) \rangle_\lambda}{\langle W(\lambda) \rangle_\lambda}, \quad W(\lambda) = \left(\frac{\det \mathcal{M}_{ud,0}}{\det \mathcal{M}_{ud,\lambda}} \right)^{1/4} \approx \exp\left(-\frac{\lambda V}{2T} \pi^\pm\right). \quad (13)$$

In Figure 5 we show the values of improved and unimproved pion condensate at the point close to $\mu/m_\pi = 0.5$ together with an extrapolation of the improved condensate to $\lambda = 0$. We can see that the improved pion condensate value is much smaller and less sensitive to the λ than the unimproved condensate. This picture can be compared with the extrapolation done in Figure 6 (top) in [7], which has a similar behavior for large λ , but also provides enough data points at small λ to actually perform the extrapolation of both the unimproved and improved pion condensates and confirm that

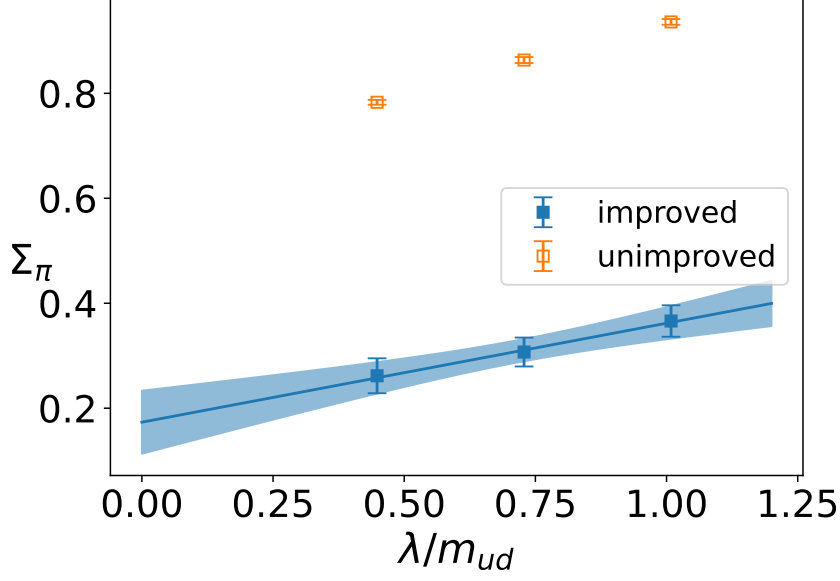


Figure 5: Extrapolation of the improved and unimproved pion condensate to $\lambda = 0$ at $T = 114$ MeV, $\mu/m_\pi = 0.54$.

they reach the same value at $\lambda = 0$. Since in that study the linear extrapolation of the improved pion condensate worked well for $\lambda/m_{ud} \leq 1.3$, we rely on it also in this study.

4. Results and summary

In Figure 6 we show our preliminary results on the value of the pion condensate and the location of the pion condensation line at four different values of the temperature. The interpolation was done using a cubic polynomial for the temperatures where we have enough points ($T = 114$ MeV, 132 MeV), and a quadratic polynomial otherwise. Location of the transition point was determined as a point where the interpolation line intersects zero. In all cases all points giving a positive value of the pion condensate were included in the fit. The error estimates for the fit line and the transition point were obtained by taking the standard deviation of the fit result for 100 simulated sets of condensate values normally distributed around the “true” values with the known standard deviation.

The results show that the vertical direction of the pion condensation line is preserved when going to smaller light quark masses, preferring the scenario shown in the left panel of the Figure 2: the location of the condensation line is compatible with the zero temperature location $\mu = m_\pi/2$.

As mentioned earlier, these results are based on the linear extrapolation to $\lambda = 0$ from the data measured at nonzero values of the pion source parameter. To be able to check the validity of this extrapolation, we are currently performing further simulations at smaller values of λ . Additionally, a T scan at several values of $\mu_I > m_\pi/2$ is being performed in order to locate the “horizontal” part of the pion condensation line as well.

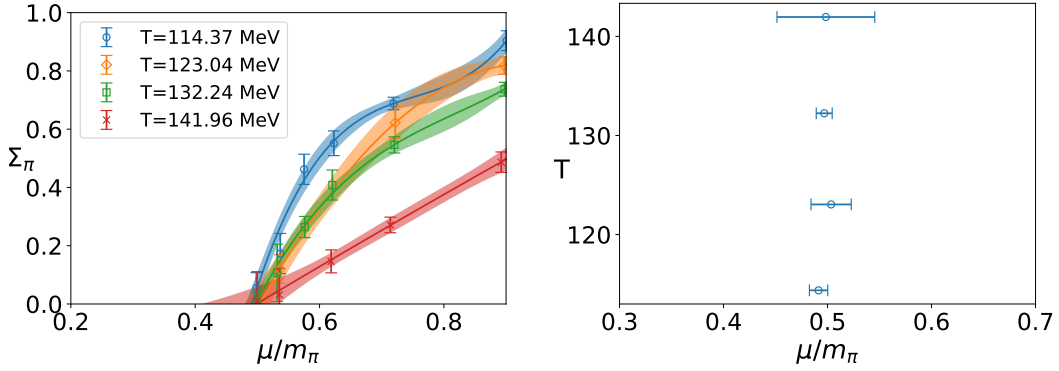


Figure 6: The value of the improved pion condensate (left) and the location of the pion condensation point (right) for four different values of temperature, obtained from the $24^3 \times 8$ lattice (no continuum extrapolation).

Acknowledgments

This work was supported by the Deutsche Forschungsgemeinschaft (DFG, German Research Foundation) – project number 315477589 – TRR 211. The authors acknowledge the use of the Goethe-HLR cluster and thank the computing staff for their support.

References

- [1] Y. Aoki, G. Endrődi, Z. Fodor, S. Katz, K. Szabo, *The Order of the quantum chromodynamics transition predicted by the standard model of particle physics*, *Nature* **443** (2006) 675 [arXiv:hep-lat/0611014]
- [2] F. Cuteri, O. Philipsen, A. Sciarra, *On the order of the QCD chiral phase transition for different numbers of quark flavours*, *JHEP* **11** (2021) 141 [arXiv:2107.12739]
- [3] P. de Forcrand, *Simulating QCD at finite density*, *PoS LAT2009* (2009) 010 [arXiv:1005.0539]
- [4] K. Nagata, *Finite-density lattice QCD and sign problem: Current status and open problems*, *Prog.Part.Nucl.Phys.* **127** (2022) 103991 [arXiv:2108.12423]
- [5] V. Vovchenko, B. B. Brandt, F. Cuteri, G. Endrődi, F. Hajkarim and J. Schaffner-Bielich, *Pion Condensation in the Early Universe at Nonvanishing Lepton Flavor Asymmetry and Its Gravitational Wave Signatures*, *Phys. Rev. Lett.* **126** (2021) no.1, 012701 [arXiv:2009.02309].
- [6] D. Son, M. Stephanov, *QCD at finite isospin density*, *Phys.Rev.Lett.* **86** (2001) 592 [arXiv:hep-ph/0005225]
- [7] B. Brandt, G. Endrődi, S. Schmalzbauer, *QCD phase diagram for nonzero isospin-asymmetry*, *Phys.Rev.D* **97** (2018) 5, 054514 [arXiv:1712.08190]
- [8] B. Brandt, G. Endrődi, *Reliability of Taylor expansions in QCD*, *Phys.Rev.D* **99** (2019) 5, 014518 [arXiv:1810.11045]

- [9] B. Brandt, F. Cuteri, G. Endrődi, S. Schmalzbauer, *Exploring the QCD phase diagram via reweighting from isospin chemical potential*, *PoS LATTICE2019* (2019) 189 [[arXiv:1911.12197](https://arxiv.org/abs/1911.12197)]
- [10] L. He, M. Jin, P. Zhuang, *Pion Superfluidity and Meson Properties at Finite Isospin Density*, *Phys.Rev.D* **71** (2005) 1160001 [[arXiv:hep-ph/0503272](https://arxiv.org/abs/hep-ph/0503272)]
- [11] E. Svanes, J. Andersen, *Functional renormalization group at finite density and Bose condensation*, *Nucl.Phys.A* **857** (2011) 16 [[arXiv:1009.0430](https://arxiv.org/abs/1009.0430)]